Green Chemistry

PAPER

View Article Online
View Journal

Cite this: DOI: 10.1039/d4gc01799d

Green method of synthesizing L-malate from D-glucose *via* CO_2 fixation using an ATP-free *in vitro* synthetic enzymatic biosystem†

Lin Fan,[a,b] Shangshang Sun,[a] Zhidan Zhang,[c] Yanmei Qin,[a] Peter Ruhdal Jensen*[d] and Chun You *‡[a,b]

In conjunction with the pressing global issue of climate change and the associated concern over global warming, increasing interest has emerged in the exploration of carbon dioxide (CO_2) as a resource for the generation of a diverse array of products intended to serve societal needs. This study presents the development of an ATP-free and NAD-balanced *in vitro* synthetic enzymatic biosystem (*iv*SEB), which comprises only five cascade thermophilic enzymes, designed for the synthesis of L-malate through CO_2 fixation powered by the utilization of D-glucose as a substrate. This designed ivSEB yields two moles of L-malate from one mole of D-glucose and two moles of CO_2. Through meticulous refinement of reaction conditions and enzyme loading amounts, this *iv*SEB has demonstrated its capability to produce 6.85 mM of L-malate *via* CO_2 fixation from an initial 5 mM of D-glucose with a molar product yield of 68.5%, and 2.45 mM of L-lactate as a byproduct. In the pursuit of assessing the industrial feasibility of this *iv*SEB, the study further subjected the system to the utilization of a high concentration (45.70 mM) of D-glucose. Although this endeavor necessitates additional optimization for enhanced efficiency, the present findings herald the emergence of an alternative avenue for the sustainable production of L-malate through CO_2 fixation, thus bearing substantial promise for addressing ecological and industrial imperatives.

Received 12th April 2024,
Accepted 22nd July 2024

DOI: 10.1039/d4gc01799d

rsc.li/greenchem

1. Introduction

As the phenomenon of global warming escalates, a growing apprehension among the scientific community revolves around a pivotal conundrum: the effective conversion of surplus carbon dioxide (CO_2) into chemical fuels, nutritional food, or daily necessities essential for societal functioning. *i.e.*, "turning waste into precious".[1] It is projected that energy-related CO_2 emissions will reach an estimated 37 billion tonnes (Gt) by the year 2025 (https://www.iea.org/topics/climatechange/). A multitude of catalysts has been developed for diverse methodologies encompassing thermochemical, photochemical, and electrochemical processes to facilitate the conversion of CO_2 into various chemical entities, such as methanol, methane, CO, and others.[2] Nevertheless, the chemical reduction of CO_2 poses a substantially intricate challenge due to the high energy demand associated with the rupture of high-energy C═O bonds, necessitating this feat to be accomplished in the absence of any externally applied potential. This challenge is further compounded by the imperative to adhere to the tenets of green chemistry. Additionally, issues pertaining to the selectivity of products and the transformation of CO_2 into longer-chain carbon chemicals continue to impose limitations on the practical implementation of the chemical systems intended for CO_2 conversion.[3]

The biological fixation of CO_2 stands as a promising alternative, characterized by its notable attributes of high selectivity, amenable reaction conditions, and ease of scalability, rendering it a significant focus for future endeavors. Plant photosynthesis constitutes the principal mechanism for natural atmospheric CO_2 fixation, however, it entails substantial land and water resources and exhibits inefficiencies in solar energy utilization.[4,5] Natural photoautotrophic microorganisms exhibit heightened rates of CO_2 fixation, and a multitude of natural photoautotrophic and heterotrophic microorganisms have undergone genetic modifications to facilitate the fixation of CO_2 into various chemicals, such as lipids,[6] biodiesel,[7] ethanol,[8] lactate,[9] 2,3-butanediol[10] and ethylene.[11]

[a]Tianjin Institute of Industrial Biotechnology, Chinese Academy of Sciences, Tianjin Airport Economic Area, Tianjin, 300308, China. E-mail: you_c@tib.cas.cn
[b]University of Chinese Academy of Sciences Sino-Danish College, Beijing, China
[c]Key Laboratory of Systems Microbial Biotechnology, Tianjin Institute of Industrial Biotechnology, Chinese Academy of Sciences, 300308 Tianjin, China
[d]Microbial Biotechnology & Biorefining National Food Institute, Kemitorvet, 201, 213, 2800 Kgs. Lyngby, Denmark. E-mail: perj@food.dtu.dk

†Electronic supplementary information (ESI) available. See DOI: https://doi.org/10.1039/d4gc01799d

‡Current address: Institute of Bioengineering, College of Chemical and Biological Engineering, Zhejiang University, Hangzhou, 310027 Zhejiang, China, E-mail: cyou@zju.edu.cn

However, it is imperative to acknowledge that microbial fermentation-based methods possess their share of limitations, such as the reduced product yields due to the requirement of a carbon source for cellular biomass synthesis, intricacies in metabolic regulation, the adverse impact of multiple gene knockouts, and the requisite development of production strains capable of withstanding the possible stresses arising from the product and extraneous environmental factors.

In vitro synthetic enzymatic biosystem (*iv*SEB), originating from cell-free synthesis (CFS),[12] has been referred to by various names in the literature, including cell-free synthetic (enzymatic) pathway biotransformation (SyPaB),[13,14] cell-free metabolic engineering,[15,16] synthetic metabolic engineering,[17] *in vitro* synthetic biology,[18,19] synthetic biochemistry,[20,21] systems biocatalysis,[22] *in vitro* biocatalytic cascade,[23,24] and artificial *in vitro* metabolism.[22,25] It has emerged as a promising biomanufacturing system, distinguished by many merits including simple operation, facile regulation, fast reaction rate, heightened transformation efficiency, and tolerance to toxicity.[26] These *in vitro* platforms have been extensively harnessed for the synthesis of various chemicals, encompassing inositol,[27] mannose,[28] glucosamine,[29] glucaric acid (GA),[30] human milk oligosaccharides (HMOs),[31] hydrogen[32] and bioelectricity.[33] Recently, several *iv*SEBs have been designed and constructed specifically for the fixation of CO_2. A common feature in most of these *iv*SEBs is a carboxylation step, entailing the integration of CO_2 into existing molecules to yield new chemical entities with an additional carbon moiety. For example, Tobias J. Erb *et al.* reported an innovative *iv*SEB termed the CETCH cycle for CO_2 fixation, showcasing a superior efficiency compared to the Kelvin carbon fixation cycle, with a CO_2-fixation rate of 5.2 ± 0.2 mM min^{-1} mg^{-1} Chl. The platform mimics the function of chloroplasts by building a light-driven ATP and NADPH regeneration module that provides energy and reducing power for the *iv*SEB-catalyzed conversion of CO_2 to polycarbons (*i.e.*, ethanolates) (carboxylation steps in the pathway include CO_2 fixation on crotonyl-CoA to generate methylmalonyl-CoA and ATP-driven fixation of HCO_3^- on propionyl-CoA to produce methylmalonyl-CoA).[34] Meanwhile, they also constructed the HOPAC cycle (version 4.0), which contains 11 enzymes from 6 different organisms, to efficiently convert CO_2 to glycolate.[35] Liao and collaborators developed a cell-free and self-replenishing CO_2-fixation system, involving a synthetic reduced glyoxylate and pyruvate synthesis (rGPS) cycle and a malonyl coenzyme A glycolate (MCG) pathway. This innovative configuration employs CO_2 to generate acetyl coenzyme A (CoA) and pyruvate and to control the regeneration of coenzymes through a sensing module (carboxylation steps in the pathway involve immobilization of HCO_3^- on phosphoenolpyruvate to synthesize oxaloacetate and CO_2 fixation on Crotonyl-CoA to produce *S*-ethylmalonyl-CoA under NADPH reduction).[36] For the *iv*SEB without a carboxylation step, an interesting *iv*SEB proposed by Ma *et al.* remarkably achieves the conversion of CO_2 to starch at a rate of 22 nmol min^{-1} mg^{-1}.[37] This particular system exhibits an impressive energy conversion efficiency in converting solar energy into starch, surpassing natural photosynthetic carbon sequestration systems of maize by a factor of 3.5, thus transcending the limitations inherent in the natural systems.

L-Malate, alternatively known as 2-hydroxysuccinic acid, holds significant stature as a fundamental platform chemical, a pharmaceutical intermediate, and a crucial intermediate within the tricarboxylic acid (TCA) cycle.[38,39] L-Malate and its derivatives (sodium malate, butyl malate, and malic aldehyde) are commonly utilized as acidifying agents and flavorings in food and beverages,[40] and serve as precursors for synthesizing unsaturated polyester resins & coatings, detergent, and fluorescent brightener in the chemical industry.[41] Moreover, L-malate and its derivatives have extensive applications in the pharmaceutical and healthcare sectors.[42] As of 2021, the global market for L-malate has reached $180 million, with a projected forecast to exceed $310 million by 2031 (**https://www.yuanzhezixun.com/malic-acid-market-research-report/**). The anticipated annual utilization of L-malate is expected to surpass 200 000 tons in the foreseeable future.[43] The synthesis of L-malate encompasses various approaches, including extraction from natural sources, chemical synthesis,[44] microbial fermentation,[45–49] and *in vitro* enzymatic methods. The *iv*SEB, which features notable advantages lay in the facile regulatory control and relatively high product yields,[18] was constructed alternatively for L-malate production through CO_2 fixation. Ye *et al.* constructed an *iv*SEB consisting of 10 enzymes, enabling the production of L-malate from D-glucose through CO_2 fixation. Approximately 2.6 mM malate and 0.6 mM lactate from 1.8 mM D-glucose were produced within 3 hours, achieving a commendable conversion yield of approximately 60%.[50] Shi *et al.* designed an ATP-balanced *iv*SEB containing 16 enzymes for the efficient synthesis of malate using starch and CO_2 as feedstock, culminating in an impressive product yield of 95.3% relative to the initial starch.[51] However, these *iv*SEBs designed for L-malate production are not without limitations, including their reliance on ATP and the involvement of a relatively extensive ensemble of more than ten enzymes (summarized in Table 1).

In this study, we developed an *iv*SEB featuring ATP-free and NAD-balanced containing only 5 enzymes for the efficient production of L-malate from D-glucose through CO_2 fixation. This biosystem is capable of operating at a high temperature (50 °C). Following optimization of reaction conditions, this *iv*SEB yielded a final L-malate titer of 6.85 mM derived from an initial 5 mM D-glucose, corresponding to a product yield of L-malate was 68.5%. In other words, this biosystem exhibited the capacity to generate 0.46 mg of malate from 0.45 mg of D-glucose while concomitantly fixing 0.15 mg of CO_2. Furthermore, this study extended its exploration to the production of L-malate from significantly higher D-glucose concentrations, specifically up to 45.7 mM, for the purpose of investigating its potential in industrial applications. Despite the appearance of the by-product (L-lactate) due to the promiscuous activity of the CO_2-fixation enzyme, this study still lays the foundation, both theoretically and practically, for the further industrial-scale production of this CO_2 fixation pathway. This

Table 1 A comparison of different *iv*SEBs for L-malate production *via* CO_2 fixation

Substrates	Need of ATP	Theoretical molar yield[a] (%)	Substrate concentration	Reaction mode	Enzyme number	L-Malate titers	Total reaction time (h)	L-Malate production rate (g L^{-1} h^{-1})	Ref.
D-Glucose	Yes	200	1.8 mM (0.32 g L^{-1})	One pot	10	2.6 mM (0.35 g L^{-1})	3	0.12	40
Maltodextrin	Yes	200[b]	27.5 mM (4.95 g L^{-1})	One pot, (IA + 13 enzymes)[c]	14	38.6 mM (5.2 g L^{-1})	12	0.15[f]	41
				One pot, (IA + 13 enzymes + 4GT)[d]	15	49.7 mM (6.7 g L^{-1})	24		
				One pot, (IA + 13 enzymes + 4GT + PPGK)[e]	16	52.4 mM (7.0 g L^{-1})	48		
D-Glucose	No	200	5 mM (0.9 g L^{-1})	One pot	5	6.85 mM (0.9 g L^{-1})	21	0.04	This work
			45.7 mM (8.23 g L^{-1})			32 mM (4.3 g L^{-1})	21	0.21	

[a] Two molecules of L-malate could be produced from 1 molecule of D-glucose, resulting in theoretical molar yield of 200%. [b] This theoretical molar yield is calculated based on the D-glucose unit of maltodextrin. [c] IA (Isoamylase) was first used to debranch maltodextrin to enhance the utilization efficiency of maltodextrin, and then 13 enzymes were subsequently added for a one-pot reaction to convert IA-treated maltodextrin to L-malate *via* CO_2 fixation for 12 hours. [d] After reaction for 12 hours in the same pot, 4-glucanotransferase (4GT) was introduced to enhance the utilization efficiency of maltodextrin. This enzyme (4GT) could catalyze transglycosylation among maltooligosaccharides, converting maltose into longer maltodextrin that α-glucan phosphorylase (αGP) can utilize and releasing D-glucose. [e] After reaction for 24 hours in the same pot, polyphosphate glucokinase (PPGK) was added to convert the releasing D-glucose to glucose 6-phosphate (G6P) in the presence of polyphosphate for L-malate production. [f] The average L-malate production rate of the entire reaction for 48 hours, including the addition of IA, 13 enzymes, 4GT and PPGK.

is primarily due to the requirement of a limited number of enzymes within this biosystem and the concurrent advancements in enzyme design, prospecting, and engineering, which collectively augment the feasibility of this approach.

2. Materials and methods

2.1 Bacterial strains, plasmids, and reagents

All chemicals involved in the assay were reagent grade, and the standard of L-malate was purchased from Sigma-Aldrich (St Louis, MO, USA). D-Glucose, NAD(H), $NaHCO_3$, NH_4Cl, dithiothreitol (DTT), *etc*., were purchased from Sinopharm (Shanghai, China), Aladdin (Shanghai, China), and Solarbio (Beijing, China). Additionally, $NaHCO_3$ (^{13}C-label 99%) was purchased from Cambridge Isotope Laboratories, Inc. The PCR enzyme used was PrimeSTAR Max DNA Polymerase from Takara (Tokyo, Japan). *E. coli* TOP10 purchased from CWBio (Beijing, China) was used for DNA manipulation. *E. coli* BL21 (DE3) and *Rosetta* 2 (DE3) purchased from Invitrogen Co. (Carlsbad, CA, USA) were used as hosts for target protein expression. LB (Luria–Bertani) culture medium was used for strain growth and protein expression.

2.2 Cloning, expression, and purification

All the plasmids are listed in Table S1.† The three plasmids, namely, pET-28a-ssgdh encoding glucose dehydrogenase (*Ss*GDH) from *Sulfolobus solfataricus*, pET-28a-sackdga encoding 2-keto-3-deoxygluconate aldolase (*Sac*KDGA) from *Sulfolobus sacidocaldarius*, and pET-28a-taaldh encoding glyceraldehyde dehydrogenase (*Ta*ALDH) from *Thermoplasma acidophilum*, were obtained from our previous studies.[52] The DNA sequence of dihydroxy acid dehydratase (*Pu*DHAD) from *Paralcaligenes ureilyticus* (575 amino acids, WP_132585145.1) and malate dehydrogenase (*Tk*MDH) from *Thermococcus kodakarensis* (425 amino acids, BAE47514.1) with a C-terminal 6 × His tag was synthesized and subcloned into pET28a by BGI Tech (Shenzhen, China), yielding the plasmids pET-28a-pudhad and pET28a-tkmdh. Compared with the wild-type enzyme, the gene encoding MDH has three mutation sites (R221G/K228R/I310 V).[53] The mutations made this MDH more soluble in *E. coli*, reversed coenzyme specificity from $NADP^+$ to NAD^+, and reduced the proportion of byproduct, which is L-lactate.

The plasmids pET28a-ssgdh, pET-28a-pudhad, and pET28a-tkmdh were transformed into *E. coli* BL21 (DE3) for enzyme expression, while pET28a-sackdga and pET28a-taaldh were transformed into *Rosetta* 2 (DE3). The single clone containing the desired plasmids was cultivated in 100 ml LB with 100 μg mL^{-1} ampicillin or 50 μg mL^{-1} kanamycin in 1-L Erlenmeyer flasks with a rotary shaking rate of 250 rpm at 37 °C. When the OD600 reached 0.6–0.8, protein expression was induced by the addition of isopropyl-β-D-thiogalactopyranoside (IPTG) (final concentration, 0.1 mM for *Ss*GDH, *Sac*KDGA, and *Ta*ALDH, 0.2 mM for *Tk*MDH, and 0.5 mM for *Pu*DHAD). The culture was incubated at 16 °C for 18 h with a rotary shaking rate of

250 rpm. After incubation, the cells were harvested by centrifugation at 4 °C, washed, and resuspended in 50 mM HEPES buffer (pH 7.5) containing 50 mM NaCl. The cell pellets were then lysed using a Fisher Scientific Sonic Dismembrator Model 500 (3 s pulse on and off, total 360 s, at 60% amplitude) in an ice bath. Following centrifugation, the enzymes in the supernatant were purified by using Ni-NTA resin (GE, USA),[54] and the expression levels of recombinant proteins were determined by SDS-PAGE. The protein concentrations were measured by the Bradford method with bovine serum albumin as the standard. Finally, glycerol at a final concentration of 10% (v/v) was added to the protein samples and stored at −20 °C.

2.3 Enzyme activity assays

The enzyme activity assays of the five enzymes were all performed at 50 °C in 100 mM HEPES buffer (pH 7.0). The activities of *Ss*GDH,[15] *Pu*DHAD,[55] *Ta*ALDH,[56] and *Sac*KDGA[57] were measured as previously described.[52] Briefly describing, *Ss*GDH utilizes the coenzyme NAD^+ to catalyze D-glucose to generate glucose-1,5-lactone and NADH. The reaction system was operated at 50 °C in 100 mM HEPES buffer (pH 7.0) containing 50 mM D-glucose, 5 mM $MgCl_2$, 4 mM NAD^+, and 0.1 g L^{-1} *Ss*GDH. *Pu*DHAD, which is a FeS cluster-dependent enzyme, catalyzes two reactions (gluconate → 2-keto-3deoxygluconate + H_2O, glycerate → Pyruvate + H_2O) in the pathway. The first reaction system was operated at 50 °C in 100 mM HEPES buffer (pH 7.0) containing 20 mM gluconate, 5 mM $MgCl_2$, 0.25 mM NADH, 1 U ml^{-1} *Tm*LDH (L-lactate dehydrogenase from *Thermotoga maritima*), *Sac*KDGA and 0.01 g L^{-1} *Pu*DHAD. The second reaction system was operated at 50 °C in 100 mM HEPES buffer (pH 7.0) containing 1 mM glycerate, 5 mM $MgCl_2$, 0.25 mM NADH, 1 U mL^{-1} *Tm*LDH and 0.1 g L^{-1} of *Pu*DHAD. *Sac*KDGA can catalyze 2-keto-3-deoxygluconate to pyruvate and glyceraldehyde. The enzyme activity of this reaction will be determined by using gluconic acid as the substrate with excess *Pu*DHAD and *Tm*LDH. The reaction system was performed at 50 °C in 100 mM HEPES buffer (pH 7.0) containing 20 mM gluconic acid, 5 mM $MgCl_2$, 0.27 mM NADH, 2 U mL^{-1} *Pu*DHAD, 1 U mL^{-1} *Tm*LDH, and 0.1 g L^{-1} *Sac*KDGA. *Ta*ALDH can catalyze glyceraldehyde to glycerate (glyceraldehyde + NAD^+ + H_2O → glycerate + NADH + H^+). The reaction system was operated at 50 °C in 100 mM HEPES buffer (pH 7.0) containing 5 mM DL-glyceraldehyde, 5 mM $MgCl_2$, 5 mM NAD^+, and 0.1 g L^{-1} *Ta*ALDH.

The above enzymatic activity was calculated by measuring the rate of A340 linear rate of change (εNADH = 6.22 mM^{-1} cm^{-1}) in an Agilent spectrophotometer. The *Tk*MDH possesses both pyruvate carboxylating activity (Pyruvate + NADH + CO_2 → L-malate + NAD^+) and reducing activity (Pyruvate + NADH → L-lactate + NAD^+).[50] The activity of *Tk*MDH was assayed anaerobically at 50 °C in a 500 μl system comprising 5 mM pyruvate, 100 mM $NaHCO_3$, 100 mM HEPES buffer (pH 7.0), 0.5 mM $MnCl_2$, 15 mM NH_4Cl, 2 mM NADH and a certain concentration of *Tk*MDH. The solution was incubated at 50 °C for 3 min, and then pyruvate was added to initiate the reaction. The reaction was terminated by mixing an aliquot of the reaction sample with 1.88 M $HClO_4$ and then neutralizing the pH with 5 M KOH. The concentration of the product L-malate was determined by high-performance liquid chromatography (HPLC). One unit of enzymatic activity (U) was defined as the amount of enzyme required to catalyze the 1 μM corresponding product from the target substrate per minute at 50 °C.

2.4 Proof-of-concept experiments for the synthesis of L-malate

This one-pot *iv*SEB for L-malate production, which comprised 5 mM D-glucose, 100 mM HEPES-NaOH buffer (pH 7.0), 100 mM $NaHCO_3$, 5 mM $MgCl_2$, 0.5 mM $MnCl_2$, 2 mM NAD^+, 2 mM DTT, 50 mM NH_4Cl, and five thermophilic enzymes (*Ss*GDH, *Pu*DHAD, *Sac*KDGA, *Ta*ALDH, and *Tk*MDH) at a concentration of 1 U ml^{-1} for each enzyme, was performed at 50 °C under aerobic and anaerobic conditions (introduction of CO_2) with a reaction volume of 500 μl. An aliquot (65 μL) was withdrawn at specific time intervals, and 35 μl of 1.88 M $HClO_4$ was added to terminate the reaction, followed by the addition of 13.5 μl of 5 M KOH to neutralize and adjust the pH of the system. D-Glucose, gluconic acid, glyceraldehyde, glyceric acid, pyruvate, and L-malate concentrations in the reaction system were assessed using HPLC (Shimadzu, Japan) equipped with a Bio-Rad HPX-87H column and a refractive index detector. The mobile phase comprised 5 mM H_2SO_4 at a flow rate of 0.5 mL min^{-1} at 35 °C, with a single injection volume of 10–20 μL. Notably, testing for 2-keto-3-desoxygluconate was omitted due to its unavailability in the market.

2.5 The determination of ^{13}C-labeled L-malate

To confirm the sequestration of CO_2 to L-malate, the unlabelled $NaHCO_3$ in the proof-of-concept reaction system was replaced with ^{13}C-labelled $NaHCO_3$. At 50 °C for 24 h, the reaction was terminated by $HClO_4$, and the pH was neutralized with KOH. Liquid chromatography-mass spectrometry (LC-MS) was used to detect ^{13}C-labeled metabolites. For LC-MS/MS analysis, a UHPLC LC-30A system (Shimadzu, Japan) equipped with a Triple TOF 5600 mass spectrometer (Sciex, USA) was used. A zic-HILIC column (100 mm 2.1 mm, 3.5 m) was used to separate the samples (Merck, German). Water/acetonitrile/ammonium acetate (solution A: 100%/0%/10 mM, solution B: 0%/100%/0 mM) were used as solvents. The LC method was as follows: 0–3 minutes with 90% solution B, 3–25 minutes with 90–60% solution B, 25–30 minutes with 60% solution B, and 30–38 minutes with 90% solution B. A 0.3 ml min^{-1} flow rate was applied. The following were the MS parameters: ESI source; negative mode; ion voltage 4500 V; declustering potential 80 V; source temperature 55 °C: curtain gas, 35 psi; nebulizer gas, 55 psi; and heatergas, 55 psi. Each scan cycle included one TOF MS survey scan as well as 15 MS/MS scans. The mass ranges for TOF MS were *m*/*z* 50–1200, and those for LC/MS were *m*/*z* 30–1200. The IDA (information-dependent acquisition) function of the Analyst TF 1.6 software (Sciex, USA) was used to control the acquisition of MS/MS spectra with dynamic

background subtraction. The mass accuracy was calibrated using an automated calibrant delivery system (Sciex, USA) connected to the DuoSpray source's second inlet.[58]

2.6 Optimization of the reaction conditions

2.6.1 Effect of buffer types on L-malate production. The effects of different buffer types on the production of L-malate in the reaction system were evaluated. A 500 μl anaerobic reaction system (aerate CO_2 until anaerobic indicated by resazurin) in buffers with different pH values, such as HEPES–NaOH (pH 7.0–8.0), MOPS (pH 6.5–8.0), Tris-HCl (pH 7.0–8.0), citrate (pH 6.0–6.5) and K_2HPO_4–KH_2PO_4 (pH 6.0–8.0) containing 5 mM D-glucose, 100 mM $NaHCO_3$, 5 mM $MgCl_2$, 0.5 mM $MnCl_2$, 2 mM NAD^+, 2 mM DTT (dithiothreitol), 50 mM NH_4Cl, and 1 U ml^{-1} enzymes (*Ss*GDH, *Pu*DHAD, *Sac*KDGA, *Ta*ALDH, and *Tk*MDH). The reaction was carried out at 50 °C for 20 h, and the yield of L-malate under the action of different types of buffers was determined by HPLC.

2.6.2 Effect of buffer concentration on L-malate production. The effect of different concentrations of K_2HPO_4–KH_2PO_4 buffer (pH 6.5), NH_4Cl, and $NaHCO_3$ on L-malate yield was tested. The 500 μl anaerobic reaction systems were performed in different concentrations of K_2HPO_4–KH_2PO_4 buffer (pH 6.5) (10, 30, 50, 100, 200, and 400 mM), NH_4Cl (0, 10, 30, 50, 100, 200), and $NaHCO_3$ (0, 10, 30, 50, 100, 200) containing 5 mM D-glucose, 5 mM $MgCl_2$, 0.5 mM $MnCl_2$, 2 mM NAD^+, 2 mM DTT, and 1 U ml^{-1} enzymes (*Ss*GDH, *Pu*DHAD, *Sac*KDGA, *Ta*ALDH, and *Tk*MDH). The reactions were carried out at 50 °C for 20 h, and the concentrations of L-malate under the action of different buffer concentrations were determined by HPLC.

2.6.3 Effect of coenzyme and enzyme concentrations on L-malate production. The effects of loading amounts of thermophilic enzymes on the production of L-malate in the reaction system were optimized by titration method.[59] The 500 μl anaerobic reaction system was performed in 50 mM K_2HPO_4–KH_2PO_4 buffer (pH 6.5) containing 5 mM D-glucose, 100 mM $NaHCO_3$, 5 mM $MgCl_2$, 2 mM NAD^+, 0.5 mmol L^{-1} $MnCl_2$, 2 mM DTT, 30 mM NH_4Cl, and different enzyme concentrations. The reactions were carried out at 50 °C for 20 h followed by the determination of L-malate concentration by HPLC. For the optimization of MDH loading amount, the reactions were performed under the same loading concentration of KDGA, ALDH, GDH, DHAD, and NAD^+ with the proof-of-concept experiment, and different concentrations of MDH (0–4 U ml^{-1}) were tested for L-malate production. The minimum enzyme loading of MDH that can maximize L-malate production was settled for the optimization of the loading amount of KDGA (0–3 U ml^{-1}). When the optimal enzyme loading of MDH and KDGA were settled, the optimal enzyme loading of ALDH from 0–3 U ml^{-1} was determined, followed by GDH (0–3 U ml^{-1}), and DHAD (0–3 U ml^{-1}). After optimal loading amounts of the five enzymes were confirmed, the concentration of NAD^+ was varied from 0 to 6 mM for optimization.

2.7 L-Malate production under optimal reaction conditions and high concentration of D-glucose

In an anaerobic vial, CO_2 was introduced to remove oxygen from the solution and the reaction was conducted in 50 mM KH_2PO_4–K_2HPO_4 buffer (pH 6.5) comprising 100 mM $NaHCO_3$, 30 mM NH_4Cl, 2 mM DTT, 5 mM $MgCl_2$, 0.5 mM Mn^{2+}, 2.0 mM NAD^+, 1.0 U mL^{-1} GDH, 1.5 U mL^{-1} DHAD, 1.0 U mL^{-1} KDGA, 1.5 U mL^{-1} ALDH, and 1.2 U mL^{-1} MDH. 5 mM D-glucose was spiked to start the system, and an aliquot of the reaction sample was withdrawn at different time point at 50 °C (0, 2, 4, 8, 21, and 24 h) for the determination of the concentrations of D-glucose, L-malate and L-lactate.

L-Malate was synthesized using a high concentration of D-glucose to investigate the industrialization potential of the system. A one-pot biosynthesis was performed under equivalent anaerobic conditions as described above with 50 mM KH_2PO_4–K_2HPO_4 buffer (pH 6.5) containing 45 mM D-glucose (9-fold higher concentration than that described in section 2.4) at 50 °C, and the enzyme loading was 10-fold scaled up. Because of the limitations of the reaction volume and pH, the addition of $NaHCO_3$ only increased to 200 mM, and other reagent levels were kept constant. An aliquot (65 μl) of the reaction sample was taken at different time points. The concentrations of D-glucose, L-malate, and L-lactate in the reaction solution were determined as described above.

3. Results

3.1 Design of an *iv*SEB for the production of L-malate from D-glucose *via* CO_2 fixation

An *iv*SEB employing a minimal ensemble of five enzymes for the production of L-malate using D-glucose and CO_2 as substrates was devised (Fig. 1A), including D-glucose dehydrogenase (GDH), 2-keto-3-deoxygluconate aldolase (KDGA), glyceraldehyde dehydrogenase (ALDH), dihydroxy acid dehydratase (DHAD), and malate dehydrogenase (MDH). GDH catalyzed the conversion of D-glucose into gluconate, concurrently generating 1 NADH from 1 NAD^+. Subsequently, DHAD converts gluconate to 2-keto-3-deoxygluconate, which is subsequently converted to pyruvate and glyceraldehyde by KGDA. In sequence, ALDH converts glyceraldehyde to glycerate, resulting in the generation of 1 NADH from 1 NAD^+. It is noteworthy that DHAD also plays a role in the dehydration of glycerate to yield pyruvate. Finally, MDH converts pyruvate and CO_2 to L-malate, concomitantly consuming 1 NADH and producing 1 NAD^+. As a result, 2 molecules of L-malate are synthesized from 1 molecule of D-glucose and 2 molecules of CO_2, thereby ensuring the meticulous balance of the NAD^+/NADH coenzyme pool within this biosystem. The Gibbs free energy (ΔG°) of the overall route, which was analyzed using the eQuilibrator website (**https://equilibrator.weizmann.ac.il/**), is −175.8 ± 12.1 kJ mol^{-1} at pH 7.5 and the ionic strength of 0.25 M (Fig. 1B), and the ΔG° of the last step of converting pyruvate and CO_2 to L-malate is −12.1 ± 6.1 kJ mol^{-1}. This computation signifies that, in the presence of an excess of CO_2, the product yield of L-malate

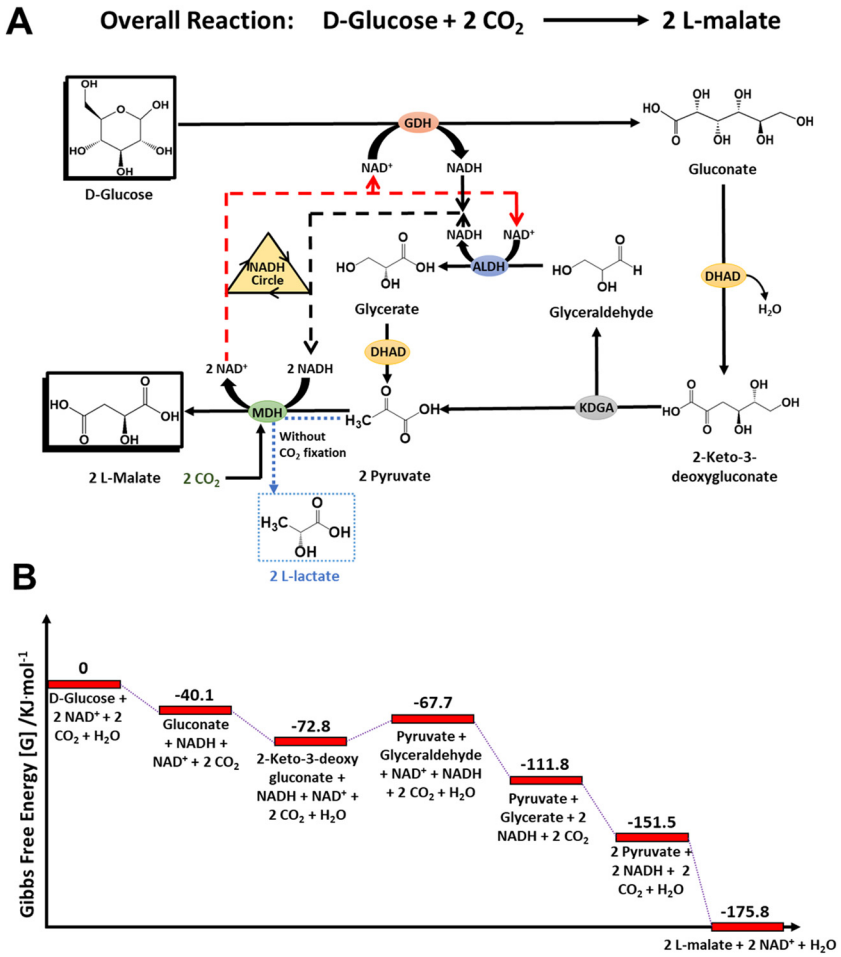

Fig. 1 (A) Diagram of an *in vitro* synthetic enzymatic biosystem (*iv*SEB) for the conversion of D-glucose to L-malate *via* CO_2 fixation. Abbreviations: GDH, glucose dehydrogenase; DHAD, dihydroxy acid dehydratase; KDGA, 2-keto-3-desoxygluconate aldolase; ALDH, glyceraldehyde dehydrogenase; MDH, malate dehydrogenase; NADH, reduced nicotinamide adenine dinucleotide; NAD^+, oxidized nicotinamide adenine dinucleotide. L-Lactate could be produced from pyruvate catalyzed by MDH in this study without CO_2 fixation. (B) The changes in Gibbs free energy for each individual reaction of this *iv*SEB under conditions characterized by a pH of 7.5 and an ionic strength of 0.25 M (https://equilibrator.weizmann.ac.il/).

derived from D-glucose should approach nearly 100%, underscoring the thermodynamic favorability of this conversion process.

3.2 Determination of L-malate and other compounds involved in the *iv*SEB

Based on HPLC results, L-malate exhibited a retention time of approximately 12.0 min, while D-glucose, gluconate, pyruvate, glycerate, and glyceraldehyde had retention times of approximately 10.7, 10.9, 11.7, 13.4, and 13.4 min, respectively (Fig. S1†). This distinction in retention times demonstrates the effective capability of HPLC in distinguishing L-malate from other intermediates. Additionally, the concentration of L-malate and L-lactate was quantified using HPLC, with concentration showing a direct proportionality to peak intensity values (Fig. S2†).

3.3 Enzyme purification and enzyme activity assays

We exclusively selected enzymes from thermophilic microorganisms for this study (Table 2). This choice was driven by the practical advantages of simplifying enzyme purification through a straightforward heat treatment process, making it particularly suitable for industrial applications. In a previous publication,[52] we detailed the utilization of GDH from *Sulfolobus solfataricus* (*Ss*GDH), KDGA from *Sulfolobus sacidocaldarius* (*Sac*KDGA), and ALDH from *Thermoplasma acidophilum* (*Ta*ALDH). Additionally, DHAD from *Paralcaligenes ureilyticus* (*Pu*DHAD) exhibited high activity on glycerate,[55] and MDH from *Thermococcus kodakarensis* (*Tk*MDH) was chosen for its crucial thermal stability and coenzyme preference for NAD^+.[53] All purified enzymes underwent SDS-PAGE analysis, revealing molecular weights of approximately 41.7 kDa for *Ss*GDH, 59.4 kDa for *Pu*DHAD, 32.5 kDa for *Sac*KDGA, 54.7 kDa for *Ta*ALDH, and 50.0 kDa for *Tk*MDH, consistent with their predicted values (Fig. S3†).

Table 2 List of enzymes and some of the basic information of these enzymes

Abbreviation	Enzyme	Source	EC.	Opt. T (°C)	Reaction	Specific activity[a] (U mg^{-1})
GDH	Glucose dehydrogenase	*Sulfolobus Solfataricus*	1.1.1.47	70[52]	D-Glucose + NAD^+ → D-glucono-1,5-lactone + NADH + H^+	12.3
DHAD	Dihydroxy acid dehydratase	*Paracaligenes ureilyticus*	4.2.1.9	55[67]	(1) D-Gluconate → 2-keto-3-deoxygluconate + H_2O (2) Glycerate → Pyruvate + H_2O	130 1.3
KDGA	2-Keto-3-desoxygluconate aldolase	*Sulfolobus acidocaldarius*	4.1.2.14	99[15]	2-Keto-3-deoxygluconate → Pyruvate + Glyceraldehyde	1.4
ALDH	Glyceraldehyde dehydrogenase	*Thermoplasma acidophilum*	1.2.1.3	63[52]	Glyceraldehyde + NAD^+ + H_2O → Glycerate + NADH + H^+	1.2
MDH	L-Malate dehydrogenase	*Thermococcus kodakarensis*	1.1.1.40	70[50]	Pyruvate + CO_2 + NADH + H^+ → L-malate + NAD^+	1.0[b]

[a] The specific activity of enzymes was determined at 50 °C. [b] This enzymatic activity was measured under anaerobic conditions.

The specific activity values of *Ss*GDH, *Sac*KDGA, and *Ta*ALDH were 12.3, 1.4, and 1.2 U mg^{-1} at 50 °C, respectively, while *Pu*DHAD exhibited specific activity values of 130 U mg^{-1} on gluconate and 1.3 U mg^{-1} on glycerate at 50 °C, respectively (Table 2). It is worth noting that *Tk*MDH, in addition to its primary function in the carboxylation of pyruvate and CO_2 to L-malate, also exhibited a secondary reduction reaction, converting pyruvate to L-lactate. The product of *Tk*MDH using pyruvate and CO_2 as substrates in the presence of NADH was analyzed by HPLC (Fig. S4†). As expected, *Tk*MDH can not only convert pyruvate and CO_2 to L-malate (carboxylation reaction), but also could convert pyruvate to L-lactate (reduction reaction), with a final consumption of 2.45 mM pyruvate, a final titer of 1.22 mM L-malate, and 0.56 mM L-lactate. Based on these values, the specific activity values for *Tk*MDH were calculated as 1.0 U mg^{-1} for the production of L-malate and 0.5 U mg^{-1} for the generation of L-lactate, based on the experimental data.

3.4 Proof-of-concept experiment for converting D-glucose to L-malate *via* CO_2 fixation

Because the retention times for D-glucose and gluconate (10.7 and 10.9 min, respectively) are similar, a glucose kit was adopted for the quantification of substrate consumption during the reaction. The reaction temperature of the proof-of-concept experiment was set at 50 °C with 100 mM HEPES–NaOH buffer (pH 7.0) containing 5 mM D-glucose, 100 mM $NaHCO_3$, 5 mM $MgCl_2$, 2 mM DTT, 0.5 mM $MnCl_2$, 2 mmol L^{-1} NAD^+, and 1 U ml^{-1} of the five thermophilic enzymes (*Ss*GDH, *Pu*DHAD, *Sac*KDGA, *Ta*ALDH, and *Tk*MDH). According to the *iv*SEB containing *Tk*MDH constructed by H. Ohtake *et al.*, the introduction of CO_2 into the system is more favourable for the generation of L-malate.[50] To verify the effect of the two reaction environments on this *iv*SEB, two distinct reaction environments were examined, namely aerobic conditions without the introduction of CO_2 and anaerobic conditions with CO_2 aeration, respectively. In the absence of aeration of CO_2, under aerobic condition, only 1.34 mM L-malate was produced with the yield of 14.7% relative to the initial 4.52 mM D-glucose (Fig. S5†). Conversely, in the anaerobic state with aeration of CO_2, a substantially increased L-malate titer of 2.19 mM was achieved after reaction for 21 h, while 5 mM of D-glucose was consumed. Simultaneously, a smaller quantity of L-lactate (approximately 1.06 mM) was produced (Fig. 2A & B). This proof-of-concept experiment not only demonstrated the feasibility of CO_2 fixation to L-malate powered by D-glucose, but also underscored the superior suitability of the reaction system for conversion under anaerobic conditions.

3.5 Validation of CO_2 fixation to L-malate by ^{13}C labeling

To substantiate the additional carbon present in L-malate relative to pyruvate was derived from CO_2, ^{13}C-labeled $NaHCO_3$ was employed in the reaction system, and subsequent product analysis was conducted utilizing liquid chromatography-mass spectrometry (LC-MS) (Fig. S6†). To maintain an anaerobic

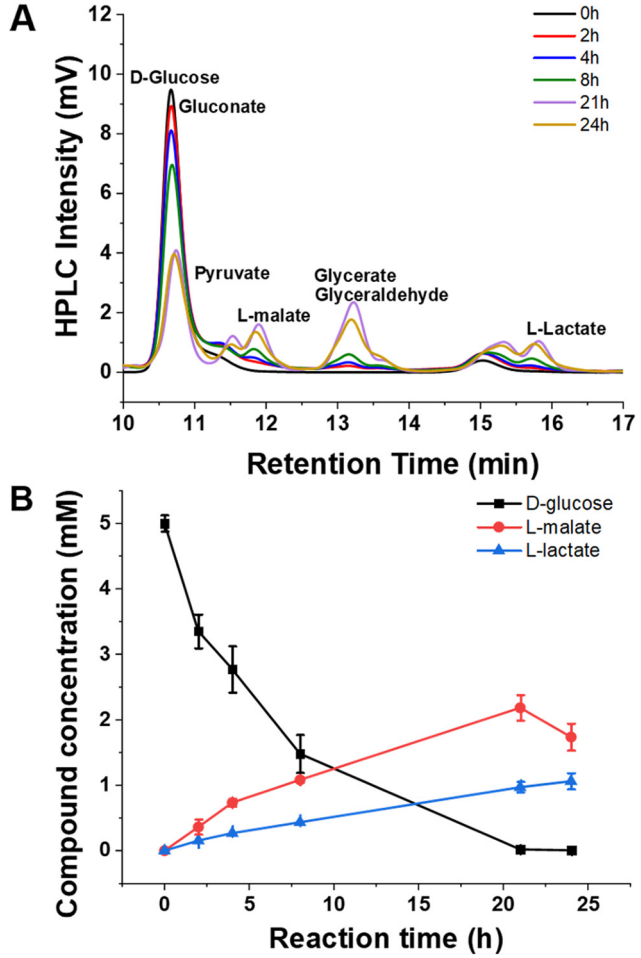

Fig. 2 The proof-of-concept experiment for the production of L-malate from D-glucose *via* CO_2 fixation by an *iv*SEB in the anaerobic state. (A) HPLC profiles of the proof-of-concept experiment under anaerobic conditions. (B) The concentration profiles of D-glucose (square), L-malate (circle), and L-lactate (triangle). The reaction was performed at 50 °C in the anaerobic state with aeration of CO_2 in 100 mM HEPES–NaOH buffer (pH 7.0) containing 100 mM $NaHCO_3$, 5 mM D-glucose, 5 mM $MgCl_2$, 0.5 mM $MnCl_2$, 2 mM DTT, 50 mM NH_4Cl, 1.0 U mL^{-1} GDH, 1.0 U mL^{-1} DHAD, 1.0 U mL^{-1} KDGA, 1.0 U mL^{-1} ALDH, 1.0 U mL^{-1} MDH, and 2.0 mM NAD^+. Values shown are means of triplicate determinations.

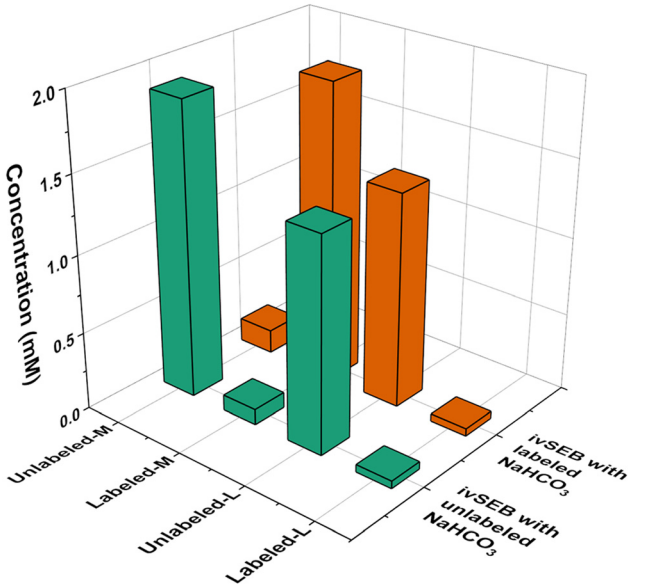

Fig. 3 ^{13}C-labeled and unlabeled L-malate and L-lactate produced by our *iv*SEB supplied with ^{13}C-labeled or unlabeled $NaHCO_3$. Unlabeled-M and unlabeled-L represent unlabeled malate and lactate, while labeled-M and labeled-L represent the ^{13}C-labeled malate and lactate, respectively. The reactions were performed in 100 mM HEPES–NaOH buffer (pH 7.0) at 50 °C under anaerobic conditions (aeration of N_2) containing 5 mM D-glucose, 100 mM ^{13}C-labeled or unlabeled $NaHCO_3$, 50 mM NH_4Cl, 2 mM DTT, 5 mM $MgCl_2$, 0.5 mM Mn^{2+}, 2.0 mM NAD^+, 1.0 U mL^{-1} GDH, 1.0 U mL^{-1} DHAD, 1.0 U mL^{-1} KDGA, 1.0 U mL^{-1} ALDH, and 1.0 U mL^{-1} MDH.

environment while averting potential interference, nitrogen gas (N_2) was employed. Upon utilizing ^{13}C-labeled $NaHCO_3$ as the substrate, the ^{13}C-labeled L-malate (1.9 mM) accounted for approximately 93% of the total L-malate produced. In contrast, when unlabeled $NaHCO_3$ was used as the substrate, the proportion of ^{13}C-labeled L-malate within the L-malate pool was reduced to approximately ~4–5% (Fig. 3). During the course of these experiments, L-lactate was concurrently generated. Nevertheless, the percentage of ^{13}C-labeled L-lactate remained consistent, consistently hovering at 3%, while the concentration of unlabeled lactate was maintained at 1.38 mM (Fig. 3). These findings illuminate that CO_2 fixation process executed by our *iv*SEB culminates in the production of L-malate, whereas L-lactate emerging solely as a byproduct of the MDH's reduction of pyruvate. Furthermore, the minimal quantities of labeled L-malate and L-lactate observed in experiments involving unlabeled $NaHCO_3$ indicated that standard D-glucose and $NaHCO_3$ inherently encompass trace quantities of labeled compounds.

3.6 Optimization of reaction conditions for one-pot biosynthesis of L-malate

Given the well-established influence of reaction conditions on the product yield of an *iv*SEB,[60] our objective was to maximize L-malate production from D-glucose and an excess of CO_2 by meticulous optimization of various parameters, including buffer type and concentration, enzyme loading amount and coenzyme concentration. The optimization of following reaction condition was performed at 50 °C for 20 hunder anaerobic conditions with aeration of CO_2.

Different types of buffers (100 mM) with their corresponding pH ranges, including MOPS (pH 6.5–8.0), HEPES–NaOH (pH 7.0–8.0), Tris-HCl (pH 7.0–8.0), citrate (pH 6.0–6.5) and K_2HPO_4–KH_2PO_4 (pH 6.0–8.0), were used for the production of L-malate (Fig. 4A). The employment of K_2HPO_4–KH_2PO_4 buffer exhibited superior product yield values for L-malate when compared to the use of other buffers. Furthermore, the concentration of the K_2HPO_4–KH_2PO_4 buffer (pH 6.5) was identified as optimal at 50 mM, as it yielded the higher L-malate production under lower buffer concentration

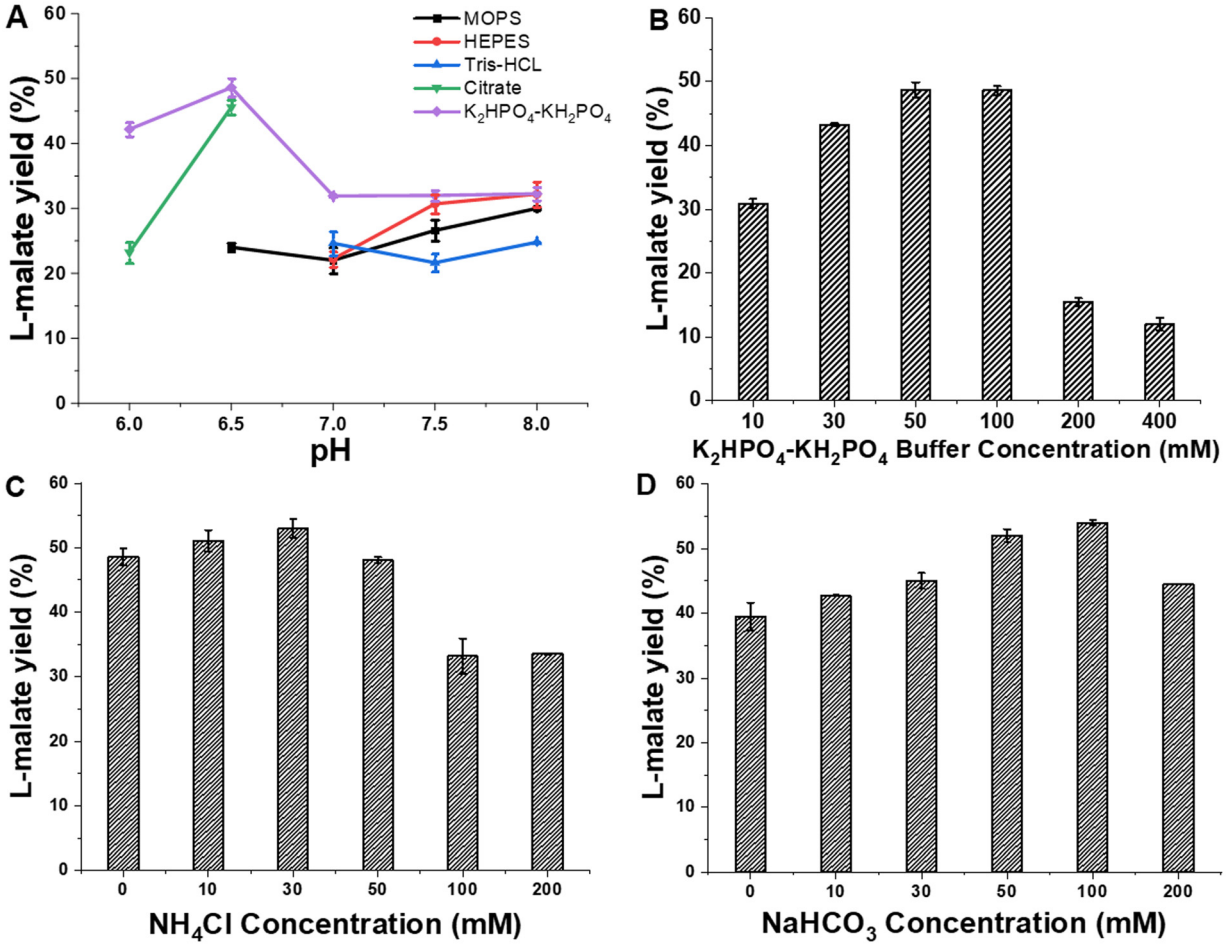

Fig. 4 Effect of pH and other reaction conditions on L-malate production from D-glucose *via* CO_2 fixation by designed *iv*SEB. (A) Effect of different buffer types and pH values, including KH_2PO_4–K_2HPO_4 buffer (pH 6.0–8.0), citrate buffer (pH 6.0–6.5), MOPS–NaOH buffer (pH 6.5–8.0), HEPES–NaOH buffer (pH 7.0–8.0), and Tris-HCl buffer (pH 7.0–8.0) on L-malate production. (B) Effect of K_2HPO_4–KH_2PO_4 buffer (pH 6.5) concentration from 10 to 400 mM on L-malate production. (C) Effect of NH_4Cl concentration from 0 to 200 mM on L-malate production. (D) Effect of $NaHCO_3$ concentration from 0 to 200 mM on L-malate production.

(Fig. 4B). In addition, the inclusion of NH_4^+ was reported to activate MDH,[53] thereby augmenting the reaction rate of the system. The optimal concentration of NH_4Cl was subsequently determined to be 30 mM (Fig. 4C). Finally, the optimal concentration of $NaHCO_3$ was established at 100 mM (Fig. 4D). It was observed that when the concentration of $NaHCO_3$ was zero, the L-malate yield still attained a commendable level of 39.6%. This outcome underscored the MDH's ability to harness gaseous CO_2 for the synthesis of L-malate, even in the absence of added bicarbonate.

The optimization of enzyme loading involved the implementation of a systematic titration method, whereby the product yields of L-malate were evaluated as each enzyme's concentration was systematically adjusted, while keeping the concentrations of the other enzymes constant. Subsequently, the minimum enzyme dosage that yielded the highest production of L-malate was identified as the optimal loading concentration. This process culminated in the optimization of the five critical enzymes in the following order: MDH, KDGA, ALDH, GDH, and DHAD. Their respective optimal loading concentrations were determined to be 1.2, 1.0, 1.5, 1.0, and 1.5 U mL^{-1}, as illustrated in Fig. 5A–5E. Following the optimization of enzyme loading amounts, the concentration of the coenzyme NAD^+ was subjected to optimization, ultimately settling at 2 mM, as depicted in Fig. 5F. Employing these meticulously established conditions, the yield of L-malate was ascertained to be 68.48%.

3.7 L-Malate production from D-glucose using CO_2 and HCO_3^- as the carbon donor

To discern the carbon source preference within our *iv*SEB concerning the production of L-malate, three distinct experimental setups were arranged as follow, (i) aeration of CO_2 exclusively, devoid of $NaHCO_3$ supplementation. (ii) Introduction of 100 mM ^{13}C-labeled $NaHCO_3$ in a deoxygenated state using N_2. (iii) Simultaneous aeration of CO_2 alongside the presence of 100 mM ^{13}C-labeled $NaHCO_3$. The concentrations of L-malate, as well as labeled L-malate, were determined. Within the first

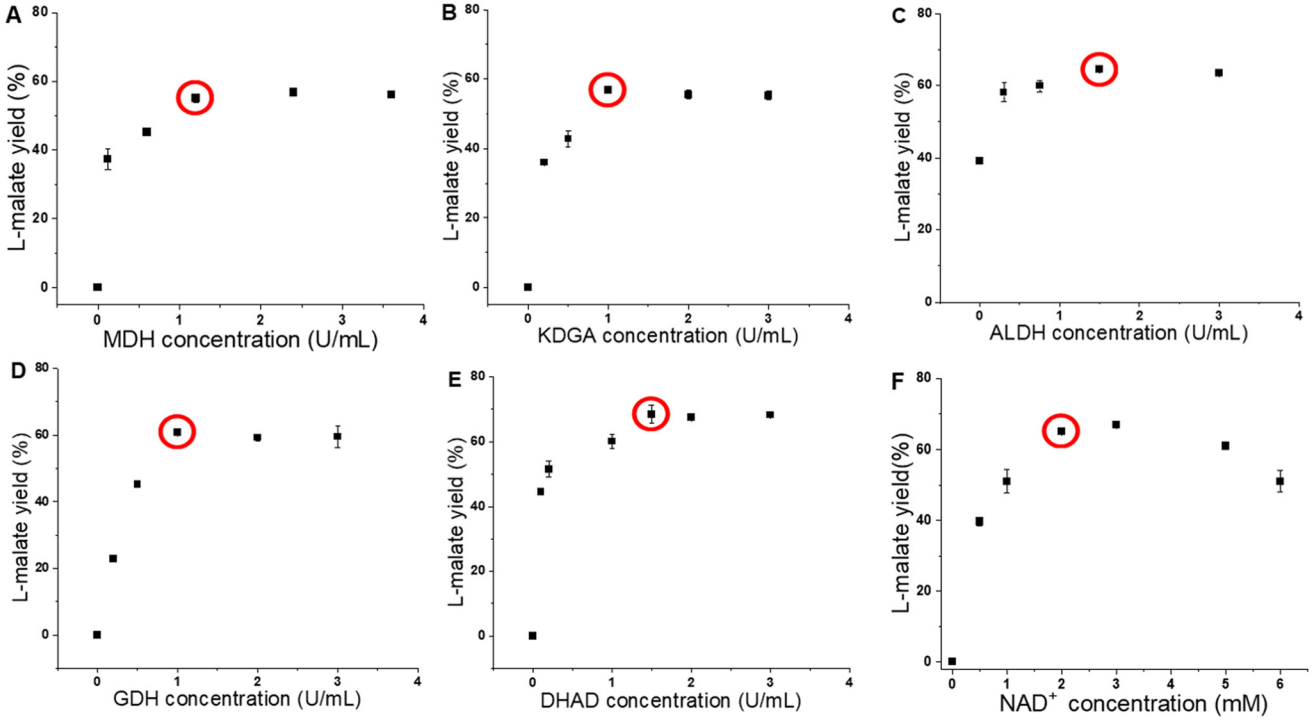

Fig. 5 Optimization of the enzymes and coenzyme concentration for L-malate production from D-glucose and CO_2. The reaction was performed in 50 mM K_2HPO_4–KH_2PO_4 buffer (pH 6.5) containing 5 mM D-glucose at 50 °C. (A) Effect of MDH concentration from 0 to 5.0 U mL^{-1} on L-malate production in the presence of 1.0 U mL^{-1} DHAD, 1.0 U mL^{-1} KDGA, 1.0 U mL^{-1} ALDH, and 1.0 U mL^{-1} GDH. (B) Effect of KDGA concentration from 0 to 5.0 U mL^{-1} on L-malate production in the presence of 1.0 U mL^{-1} GDH, 1.0 U mL^{-1} DHAD, 1.0 U mL^{-1} ALDH, and 1.2 U mL^{-1} MDH. (C) Effect of ALDH concentration from 0 to 3.0 U mL^{-1} on L-malate production in the presence of 1.0 U mL^{-1} GDH, 1.0 U mL^{-1} DHAD, 1.0 U mL^{-1} KDGA, and 1.2 U mL^{-1} MDH. (D) Effect of GDH concentration from 0 to 5.0 U mL^{-1} on L-malate production in the presence of 1.0 U mL^{-1} DHAD, 1.0 U mL^{-1} KDGA, 1.5 U mL^{-1} ALDH, and 1.2 U mL^{-1} MDH. (E) Effect of DHAD concentration from 0 to 3.0 U mL^{-1} on L-malate production in the presence of 1.0 U mL^{-1} GDH, 1.5 U mL^{-1} ALDH, 1.0 U mL^{-1} KDGA, and 1.2 U mL^{-1} MDH. (F) Effect of NAD^+ concentration from 0 to 6 mM on L-malate production. The points in the open red circle represent the optimal condition for each parameter. The values shown are the averages of three determinations.

system, the yield of L-malate was achieved at 45.6%, with 96% of the resulting L-malate being non-labeled. In the second system, the yield of L-malate exhibited an increase to 55.1%, with 94% of L-malate bearing a ^{13}C-label. The third system yielded the highest yield of L-malate, at 68.5%, and a mere 8% of the L-malate was ^{13}C-labeled (Fig. 6). These findings suggest that *Tk*MDH in our *iv*SEB exhibit a preference for gaseous CO_2 over the externally added HCO_3^- within the solution, underscoring its selective affinity for CO_2 as the primary carbon source.

3.8 Synthesis of L-malate under optimal reaction conditions from different concentrations of D-glucose

Subsequent to the aforementioned optimizations, L-malate production from D-glucose through CO_2 fixation was conducted based on these optimized conditions at 50 °C. The results, as illustrated in Fig. 7A, revealed that nearly the entire quantity of D-glucose had been consumed, with the final D-glucose concentration reaching approximately 0.07 mM after 24 hours. In this experiment, the yield of L-malate attained a level of approximately 68.5%, corresponding to 6.85 mM, and this was accomplished through the fixation of 6.85 mM CO_2. Notably, this yield represented a substantial threefold increase when compared to the proof-of-concept experiment conducted in an anaerobic environment. However, approximately 2.45 mM of L-lactate was concurrently generated. The cumulative concentration of L-malate and L-lactate amounted to 9.66 mM, and the D-glucose conversion yield reached 93%.

To investigate the industrial viability of this ATP-free (*iv*SEB for L-malate production *via* CO_2 fixation), we employed an approximately nine-fold increase in the concentration of D-glucose (reaching 45.70 mM) as the substrate. Correspondingly, the concentrations of all enzymes within the system were elevated by a factor of ten. However, due to system capacity constraints, the concentration of $NaHCO_3$ was doubled, while the concentrations of other components, such as NH_4Cl, DTT, $MgCl_2$, $MnCl_2$, and NAD^+, remained unchanged. As depicted in Fig. 7B, the reaction achieved equilibrium at around 21–24 hours, during which 38.3 mM of D-glucose was consumed. This resulted in a final titer of 32.2 mM of L-malate and 17.2 mM of L-lactate, while 32.2 mM of CO_2 was fixed in the process. The cumulative conversion yield, accounting for both L-malate and L-lactate, reached 54.1%, considering the initial concentration of D-glucose, and 64.6% based on the consumed D-glucose concentration.

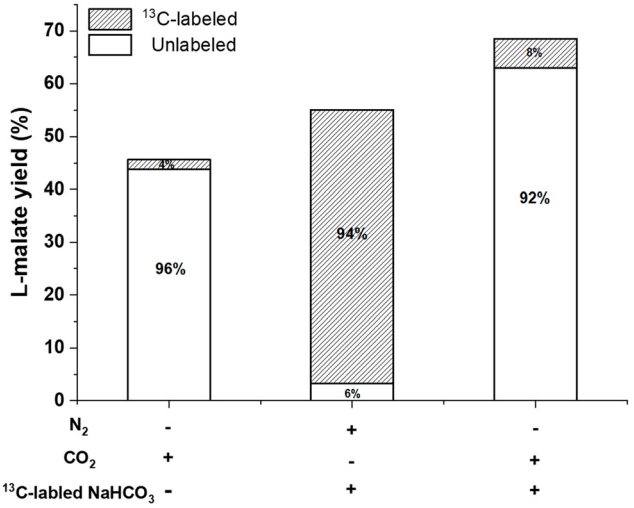

Fig. 6 The histogram of the ratio of ^{13}C-labeled/unlabeled L-malate produced by the *iv*SEB reaction system using different source of CO_2. The reactions were performed in 50 mM K_2HPO_4–KH_2PO_4 buffer (pH 6.5) at 50 °C under anaerobic conditions (aeration of CO_2/N_2) containing 5 mM D-glucose, different source of CO_2 (gaseous CO_2 only, 100 mM ^{13}C-labeled $NaHCO_3$ with aeration of N_2 and 100 mM ^{13}C-labeled $NaHCO_3$ with aeration of CO_2), 30 mM NH_4Cl, 2 mM DTT, 5 mM $MgCl_2$, 0.5 mM Mn^{2+}, 2.0 mM NAD^+, 1.0 U mL^{-1} GDH, 1.5 U mL^{-1} DHAD, 1.0 U mL^{-1} KDGA, 1.5 U mL^{-1} ALDH, and 1.2 U mL^{-1} MDH.

4. Discussion

This study has showcased the feasibility and optimization of an ATP-free *in vitro* synthetic enzymatic biosystem (*iv*SEB), consisting of a mere five enzymes, to efficiently convert D-glucose into L-malate through CO_2 fixation. In comparison to alternative *in vitro* methods,[50,51] this approach for L-malate production boasts requiring the minimum number of enzymes and being ATP-free to advance the L-malate production *via* CO_2 fixation (Table 1). Firstly, this *iv*SEB comprises only five enzymes, in contrast to a designed *iv*SEB for L-malate production from starch and CO_2, which involves more than 10 enzymes. The reduced number of enzymes within our *iv*SEB simplifies the regulation of the overall reaction, rendering it more amenable to large-scale industrial implementation. Secondly, our *iv*SEB obviates the requirement for costly ATP, different from the prior approach wherein efforts were made to balance the ADP/ATP.[51] The elimination of ATP usage is advantageous as the inherent instability of ATP can diminish reaction rates and elevate production costs.[61] Thus, despite the emergence of a byproduct resulting from the substrate promiscuity of the enzyme (*Tk*MDH) for CO_2 fixation, our *iv*SEB offers a promising avenue for CO_2 fixation in the economical synthesis of L-malate from abundant biomass sources.

Optimization of reaction conditions of our *iv*SEB successfully achieved threefold increase in the product yield of L-malate. A comparison between the optimized conditions and the proof-of-concept parameters of our *iv*SEBs highlights two primary distinctions, namely the choice of buffer type and the enzyme loading amounts. The cost-effective phosphate buffers demonstrated superior performance in terms of product yield when juxtaposed with the relatively more expensive HEPES buffers, thereby enhancing the practicality of implementing this *iv*SEB on an industrial scale. However, it is worth noting that an elevated concentration of phosphate ions did not confer any advantageous effects on the conversion process,

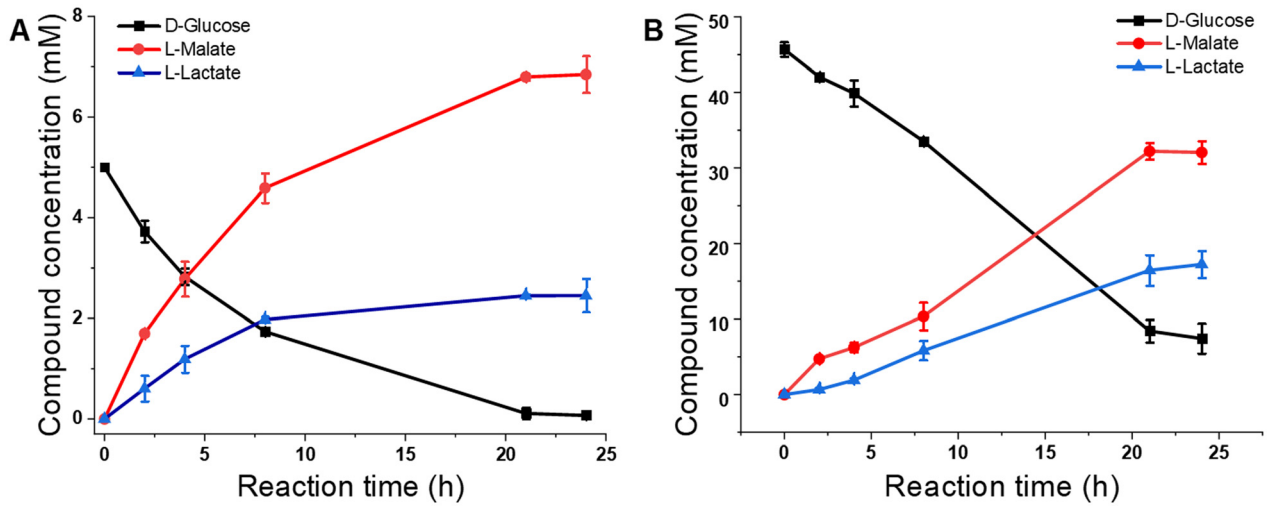

Fig. 7 L-Malate production from D-glucose *via* CO_2 fixation under optimized conditions from low concentration (A) and high concentration of D-glucose (B). (A) The reaction was performed in 50 mM K_2HPO_4–KH_2PO_4 buffer (pH 6.5) at 50 °C containing 5 mM D-glucose, 100 mM $NaHCO_3$, 30 mM NH_4Cl, 2 mM DTT, 5 mM $MgCl_2$, 0.5 mM Mn^{2+}, 2.0 mM NAD^+, 1.0 U mL^{-1} GDH, 1.5 U mL^{-1} DHAD, 1.0 U mL^{-1} KDGA, 1.5 U mL^{-1} ALDH, and 1.2 U mL^{-1} MDH under anaerobic conditions (introduction of CO_2). (B) The reaction was performed in 50 mM K_2HPO_4–KH_2PO_4 buffer (pH 6.5) at 50 °C containing 45.70 mM D-glucose, 200 mM $NaHCO_3$, 30 mM NH_4Cl, 2 mM DTT, 5 mM $MgCl_2$, 0.5 mM Mn^{2+}, 2 mM NAD^+, 10 U mL^{-1} GDH, 15 U mL^{-1} DHAD, 10 U mL^{-1} KDGA, 15 U mL^{-1} ALDH, and 12 U mL^{-1} MDH under anaerobic conditions. Values shown are means of triplicate determinations.

possibly due to the chelation of the metal ions (Mg^{2+} or Mn^{2+}) by excess phosphate ions. The optimal pH for our *iv*SEB for L-malate production was determined to be 6.5, an observation that aligns with a prior study by H. Ohtake *et al.*,[50] wherein an optimal pH of 6.5 for *Tk*MDH was identified. The conversion yield of D-glucose at low concentration could achieve to almost 100%, however, the conversion yield of D-glucose and the product yield of L-malate diminished significantly when employing higher concentrations of D-glucose for CO_2 fixation to produce L-malate. This phenomenon may be attributed to several factors, including pH fluctuations induced by elevated concentration of L-malate and L-lactate, enzyme inhibition by the accumulating product, and a reduction in the stability of some enzymes or coenzymes throughout the course of the reaction.

According to H. Ohtake *et al.*,[50] the high concentrations of $NaHCO_3$ can facilitate the production of L-malate from pyruvate *via* CO_2 fixation catalyzed by *Tk*MDH, resulting in the higher ratio of L-malate to L-lactate. However, the essential amino acid residues implicated in the interaction with CO_2/HCO_3^- have not yet been identified, and the processes of malate-enzyme-mediated pyruvate carboxylation have only scarcely been explored.[53] Interestingly, in this study, it was found that *Tk*MDH mainly utilizes gaseous CO_2 rather than HCO_3^- to generate L-malate during the carboxylation reaction. Based on its results, it is speculated that the direct substrate of *Tk*MDH is probable CO_2 rather than HCO_3^-. From a practical point of view, the direct production of malate from CO_2 is preferable to HCO_3^- because the addition of thermophilic carbonic anhydrase to facilitate the rate of CO_2 hydration can be avoided. The finding may provide an impetus for the mechanistic resolution of the reaction catalyzed by this class of enzymes.

Currently, when evaluating the cost of L-malate production *via* our *iv*SEB, the analysis based on the product titer and yield does not render it as economically competitive as conventional microbial fermentation, which yielded impressive L-malate titers of up to 181 g L^{-1} and coupled with an exemplary sugar-to-acid conversion yield of 0.99 g/g.[49] Nevertheless, given the enzyme quantity, the inherent free energy changes and the utilization of inexpensive substrates within our *in vitro* pathway, this approach holds significant potential to vie with microbial fermentation in the future. To further enhance L-malate product titer and yield in future endeavors, several strategic avenues can be explored. Firstly, the most important thing should be the gene mining and protein engineering to obtain a novel MDH with heightened substrate specificity and higher enzyme activity, enabling exclusive and effective malate production through CO_2 fixation and avoiding the production of by-products like lactate. Secondly, the construction of a multienzyme complex and the co-immobilization of all enzymes could serve to accelerate reaction rates and enhance enzyme recycling capabilities to reduce the product cost.[32,62] Thirdly, the design and implementation of an appropriate reactor, facilitating *in situ* separation of L-malate, would enable continuous production. Fourthly, the replacement of natural coenzyme (NAD) with stable biomimetic coenzymes like 1-benzyl-1,4-dihydropyridine-3-carboxamid (BNA)[63] and nicotinamide mononucleotide (NMN),[64] can contribute to stabilizing the entire *in vitro* system. Finally, the construction of recombinant microorganisms (*E. coli* or *B. subtilis*) capable of co-expressing multiple genes in one strain could further reduce the cost of enzyme production,[65] thereby facilitating the industrial process of L-malate using this *iv*SEB. Substantial efforts are needed to address various aspects, including the selection of plasmids, the order of genes if these genes were co-expressed in one plasmid, and the combination of promoter, terminator, and ribosome binding site (RBS),[66] to obtain optimized recombinant microorganisms. These strategic enhancements collectively hold promise for rendering our *iv*SEB a more competitive and economically viable option for L-malate production in the future.

In summary, we have successfully demonstrated the efficient synthesis of L-malate through the utilization of an *iv*SEB comprising a mere five enzymes, with cost-effective D-glucose and CO_2 as substrates. This study not only presents a potential scheme for the industrial-scale production of L-malate through CO_2 fixation but also offers some practical and theoretical insights that may inform the development of alternative compounds, such as oxaloacetic or succinic acid, in future research endeavors.

Data availability

The data supporting this article have been included as part of the ESI.†

Conflicts of interest

There are no conflicts to declare.

Acknowledgements

This work was supported by the National Key Research and Development Program of China (2021YFA0910601), and the National Natural Science Foundation of China (32271473, 32022044 and 32101009). The table of contents was created with BioRender.com.

References

1 O. S. Bushuyev, P. De Luna, C. T. Dinh, L. Tao, G. Saur, J. van de Lagemaat, S. O. Kelley and E. H. Sargent, *Joule*, 2018, **2**, 825–832.
2 S. C. Peter, *ACS Energy Lett.*, 2018, **3**, 1557–1561.
3 A. Modak, P. Bhanja, S. Dutta, B. Chowdhury and A. Bhaumik, *Green Chem.*, 2020, **22**, 4002–4033.
4 M. Faralli and T. Lawson, *Plant J.*, 2019, **101**, 518–528.

5 X. G. Zhu, S. P. Long and D. R. Ort, *Curr. Opin. Biotechnol.*, 2008, **19**, 153–159.
6 I. Ajjawi, J. Verruto, M. Aqui, L. B. Soriaga, J. Coppersmith, K. Kwok, L. Peach, E. Orchard, R. Kalb, W. D. Xu, T. J. Carlson, K. Francis, K. Konigsfeld, J. Bartalis, A. Schultz, W. Lambert, A. S. Schwartz, R. Brown and E. R. Moellering, *Nat. Biotechnol.*, 2017, **35**, 647–652.
7 H. Lin, Q. Wang, Q. Shen, J. Zhan and Y. Zhao, *Bioengineered*, 2013, **4**, 292–304.
8 F. Y. Liang, E. Englund, P. Lindberg and P. Lindblad, *Metab. Eng.*, 2018, **46**, 51–59.
9 S. A. Angermayr, M. Paszota and K. J. Hellingwerf, *Appl. Environ. Microbiol.*, 2012, **78**, 7098–7106.
10 M. Kanno, A. L. Carroll and S. Atsumi, *Nat. Commun.*, 2017, **8**, 14724.
11 W. Xiong, J. A. Morgan, J. Ungerer, B. Wang, P. C. Maness and J. P. Yu, *Nat. Plants*, 2015, **1**, 15053.
12 E. Buchner, *Eur. J. Inorg. Chem.*, 1897, **30**, 1110–1113.
13 Y. H. P. Zhang, *Biotechnol. Bioeng.*, 2010, **105**, 663–677.
14 Y. H. P. Zhang, J. B. Sun and J. J. Zhong, *Curr. Opin. Biotechnol.*, 2010, **21**, 663–669.
15 J. K. Guterl, D. Garbe, J. Carsten, F. Steffler, B. Sommer, S. Reisse, A. Philipp, M. Haack, B. Rühmann, A. Koltermann, U. Kettling, T. Brück and V. Sieber, *ChemSusChem*, 2012, **5**, 2165–2172.
16 Q. M. Dudley, A. S. Karim and M. C. Jewett, *Biotechnol. J.*, 2015, **10**, 69–82.
17 X. T. Ye, K. Honda, T. Sakai, K. Okano, T. Omasa, R. Hirota, A. Kuroda and H. Ohtake, *Microb. Cell Fact.*, 2012, **11**, 120.
18 J. A. Rollin, T. K. Tam and Y. H. P. Zhang, *Green Chem.*, 2013, **15**, 1708–1719.
19 S. Slomovic, K. Pardee and J. J. Collins, *Proc. Natl. Acad. Sci. U. S. A.*, 2015, **112**, 14429–14435.
20 P. H. Opgenorth, T. P. Korman and J. U. Bowie, *Nat. Commun.*, 2014, **5**, 4113.
21 J. U. Bowie, S. Sherkhanov, T. P. Korman, M. A. Valliere, P. H. Opgenorth and H. J. Liu, *Trends Biotechnol.*, 2020, **38**, 766–778.
22 W.-D. Fessner, *Nat. Biotechnol.*, 2015, **32**, 658–664.
23 M. A. Huffman, A. Fryszkowska, O. Alvizo, M. Borra-Garske, K. R. Campos, K. A. Canada, P. N. Devine, D. Duan, J. H. Forstater, S. T. Grosser, H. M. Halsey, G. J. Hughes, J. Jo, L. A. Joyce, J. N. Kolev, J. Liang, K. M. Maloney, B. F. Mann, N. M. Marshall, M. McLaughlin, J. C. Moore, G. S. Murphy, C. C. Nawrat, J. Nazor, S. Novick, N. R. Patel, A. Rodriguez-Granillo, S. A. Robaire, E. C. Sherer, M. D. Truppo, A. M. Whittaker, D. Verma, L. Xiao, Y. Xu and H. Yang, *Science*, 2019, **366**, 1255–1259.
24 E. Grandi, F. F. Özgen, S. Schmidt and G. J. Poelarends, *Angew Chem., Int. Ed.*, 2023, **62**, e202309012.
25 A. F. Kiefer, Y.-C. Liu, R. Gummerer, C. Jäger and J. Deska, *Angew. Chem., Int. Ed.*, 2023, **62**, e202301178.
26 Y.-H. P. Job Zhang, Z. Zhu, C. You, L. Zhang and K. Liu, *Synth. Biol. Eng.*, 2023, **1**, 1–37.
27 C. You, T. Shi, Y. J. Li, P. P. Han, X. G. Zhou and Y. H. P. Zhang, *Biotechnol. Bioeng.*, 2017, **114**, 1855–1864.
28 C. Y. Tian, J. G. Yang, Y. J. Li, T. Zhang, J. Li, C. X. Ren, Y. Men, P. Chen, C. You, Y. X. Sun and Y. H. Ma, *Metab. Eng.*, 2020, **61**, 215–224.
29 D. Meng, X. Wei, X. Bai, W. Zhou and C. You, *ACS Catal.*, 2020, **10**, 13809–13819.
30 Y. Li, C. You and Y.-H. P. J. Zhang, *Org. Process Res. Dev.*, 2024, **28**, 478–486.
31 M. Nishimoto and M. Kitaoka, *Biosci., Biotechnol., Biochem.*, 2007, **71**, 2101–2104.
32 E. J. Kim, J. E. Kim and Y. H. P. J. Zhang, *Energy Environ. Sci.*, 2018, **11**, 2064–2072.
33 Z. Zhu, T. Kin Tam, F. Sun, C. You and Y. H. Percival Zhang, *Nat. Commun.*, 2014, **5**, 3026.
34 T. E. Miller, T. Beneyton, T. Schwander, C. Diehl, M. Girault, R. McLean, T. Chotel, P. Claus, N. S. Cortina, J. C. Baret and T. J. Erb, *Science*, 2020, **368**, 649–654.
35 R. McLean, T. Schwander, C. Diehl, N. S. Cortina, N. Paczia, J. Zarzycki and T. J. Erb, *Sci. Adv.*, 2023, **9**, eadh4299.
36 S. Luo, P. P. Lin, L.-Y. Nieh, G.-B. Liao, P.-W. Tang, C. Chen and J. C. Liao, *Nat. Catal.*, 2022, **5**, 154–162.
37 T. Cai, H. B. Sun, J. Qiao, L. L. Zhu, F. Zhang, J. Zhang, Z. J. Tang, X. L. Wei, J. G. Yang, Q. Q. Yuan, W. Y. Wang, X. Yang, H. Y. Chu, Q. Wang, C. You, H. W. Ma, Y. X. Sun, Y. Li, C. Li, H. F. Jiang, Q. H. Wang and Y. H. Ma, *Science*, 2021, **373**, 1523–1527.
38 Z. Chi, Z. P. Wang, G. Y. Wang, I. Khan and Z. M. Chi, *Crit. Rev. Biotechnol.*, 2016, **36**, 99–107.
39 J. Iyyappan, G. Baskar, B. Bharathiraja and R. Saravanathamizhan, *Bioresour. Technol.*, 2018, **269**, 393–399.
40 W. Lu, X. Sun, L. Gao, X. Hu, H. Song and B. Kong, *Fuel*, 2022, **308**, 122012.
41 X. Yin, J. H. Li, H. D. Shin, G. C. Du, L. Liu and J. Chen, *Biotechnol. Adv.*, 2015, **33**, 830–841.
42 J. M. Glenn, M. Gray, L. N. Wethington, M. S. Stone, R. W. Stewart and N. E. Moyen, *Eur. J. Nutr.*, 2017, **56**, 775–784.
43 M. Sauer, D. Porro, D. Mattanovich and P. Branduardi, *Trends Biotechnol.*, 2008, **26**, 100–108.
44 J. H. Ahn, Y. S. Jang and S. Y. Lee, *Curr. Opin. Biotechnol.*, 2016, **42**, 54–66.
45 J. L. Yuill, *Biochem. J.*, 1928, **22**, 1504–1507.
46 E. Battat, Y. Peleg, A. Bercovitz, J. S. Rokem and I. Goldberg, *Biotechnol. Bioeng.*, 1991, **37**, 1108–1116.
47 X. Dong, X. Chen, Y. Qian, Y. Wang, L. Wang, W. Qiao and L. Liu, *Biotechnol. Bioeng.*, 2017, **114**, 656–664.
48 R. M. Zelle, E. de Hulster, W. A. van Winden, P. de Waard, C. Dijkema, A. A. Winkler, J.-M. A. Geertman, J. P. van Dijken, J. T. Pronk and A. J. A. van Maris, *Appl. Environ. Microbiol.*, 2008, **74**, 2766–2777.
49 J. Li, L. Lin, T. Sun, J. Xu, J. Ji, Q. Liu and C. Tian, *Metab. Eng.*, 2020, **61**, 416–426.
50 X. T. Ye, K. Honda, Y. Morimoto, K. Okano and H. Ohtake, *J. Biotechnol.*, 2013, **164**, 34–40.

51 T. Shi, S. Liu and Y. H. P. J. Zhang, *Metab. Eng.*, 2019, **55**, 152–160.
52 L. Xie, X. Wei, X. Zhou, D. Meng, R. Zhou, Y. P. J. Zhang, S. Xu and C. You, *Synth. Syst. Biotechnol.*, 2018, **3**, 204–210.
53 Y. Morimoto, K. Honda, X. T. Ye, K. Okano and H. Ohtake, *J. Biosci. Bioeng.*, 2014, **117**, 147–152.
54 Y. Wang, W. Huang, N. Sathitsuksanoh, Z. Zhu and Y. H. Zhang, *Chem. Biol.*, 2011, **18**, 372–380.
55 S. Sutiono, M. Teshima, B. Beer, G. Schenk and V. Sieber, *ACS Catal.*, 2020, **10**, 3110–3118.
56 F. Steffler, J. K. Guterl and V. Sieber, *Enzyme Microb. Technol.*, 2013, **53**, 307–314.
57 S. Wolterink-van Loo, M. A. Siemerink, G. Perrakis, T. Kaper, S. W. Kengen and J. van der Oost, *Archaea*, 2009, **2**, 233–239.
58 X. Lu, Y. Liu, Y. Yang, S. Wang, Q. Wang, X. Wang, Z. Yan, J. Cheng, C. Liu, X. Yang, H. Luo, S. Yang, J. Gou, L. Ye, L. Lu, Z. Zhang, Y. Guo, Y. Nie, J. Lin, S. Li, C. Tian, T. Cai, B. Zhuo, H. Ma, W. Wang, Y. Ma, Y. Liu, Y. Li and H. Jiang, *Nat. Commun.*, 2019, **10**, 1378.
59 X. L. Wei, Q. Z. Li, C. C. Hu and C. You, *Appl. Microbiol. Biotechnol.*, 2021, **105**, 1913–1924.
60 I. Ardao and A. P. Zeng, *Chem. Eng. Sci.*, 2013, **87**, 183–193.
61 J. U. Bowie, S. Sherkhanov, T. P. Korman, M. A. Valliere, P. H. Opgenorth and H. J. Liu, *Trends Biotechnol.*, 2020, **38**, 766–778.
62 R. A. Sheldon, *Adv. Synth. Catal.*, 2007, **349**, 1289–1307.
63 Y. Okamoto, V. Köhler, C. E. Paul, F. Hollmann and T. R. Ward, *ACS Catal.*, 2016, **6**, 3553–3557.
64 W. B. Black, L. Y. Zhang, W. S. Mak, S. Maxel, Y. T. Cui, E. King, B. Fong, A. S. Martinez, J. B. Siegel and H. Li, *Nat. Chem. Biol.*, 2020, **16**, 87–94.
65 H. Chen, R. Huang and Y. H. P. Zhang, *Appl. Microbiol. Biotechnol.*, 2017, **101**, 4481–4493.
66 Y. Li, S. Liu and C. You, *Biotechnol. J.*, 2020, **15**, e1900191.
67 S. Guo, X. Tan, Y. Wang, K. Li, C. Lü, C. Ma and C. Gao, *Catalysts*, 2021, **11**, 128.